

Article

Rainfall Threshold for Shallow Landslide Triggering Due to Rising Water Table

Antonello Troncone ^{*}, Luigi Pugliese  and Enrico Conte 

Department of Civil Engineering, University of Calabria, Rende, 87036 Cosenza, Italy

^{*} Correspondence: antonello.troncone@unical.it

Abstract: In the present study, a simple-to-use method is proposed for a preliminary prediction of the occurrence of shallow landslides (generally, with a thickness of 1–2 m) due to rainfall. This method can be used when a water table forms within the slope or the existing groundwater level rises due to rain infiltration, resulting in an increase in the pore water pressure. A relationship is also provided to establish when these conditions occur and the method can consequently be used. The proposed method combines a simplified solution to evaluate the change in pore water pressure within the slope due to infiltration, with the simple scheme of infinite slope to calculate a critical value of the pore water pressure that determines the incipient failure condition of the slope. In this way, a threshold curve can be also determined to readily assess whether a rainfall event with expected intensity and duration is capable of causing a slope failure at a given depth, where the initial pore water pressure is known. The method is completely analytical and only requires a few parameters as input data, which in addition can be obtained from conventional tests. A well-documented case study is considered to show how the method can be used for routine applications.

Keywords: rainfall-induced shallow landslides; groundwater; simplified method; rainfall threshold curve



Citation: Troncone, A.; Pugliese, L.; Conte, E. Rainfall Threshold for Shallow Landslide Triggering Due to Rising Water Table. *Water* **2022**, *14*, 2966. <https://doi.org/10.3390/w14192966>

Academic Editor: Stefano Luigi Gariano

Received: 30 August 2022

Accepted: 17 September 2022

Published: 21 September 2022

Publisher's Note: MDPI stays neutral with regard to jurisdictional claims in published maps and institutional affiliations.



Copyright: © 2022 by the authors. Licensee MDPI, Basel, Switzerland. This article is an open access article distributed under the terms and conditions of the Creative Commons Attribution (CC BY) license (<https://creativecommons.org/licenses/by/4.0/>).

1. Introduction

Rainfall-induced shallow landslides generally occur due to short and intense periods of rainfall or after long rainy periods, depending on soil properties and the infiltration capacity of the slope. The geometry of the unstable soil mass is usually characterized by a thickness in the order of 1–2 m, with a length per thickness exceeding 10:1 [1]. The main type of movement occurring after the failure stage is a translational slide with a direction essentially parallel to the ground surface. Nevertheless, under certain conditions, the slide may evolve into a debris flow [2–7]. As a consequence, such landslides may cause severe damage to structures and infrastructures and even fatalities. Therefore, they can be very dangerous although generally the volume of the displaced material is relatively small.

Rainfall-induced shallow landslides are often caused by the formation of a water table or an increase in the groundwater level already present within the slope before rain commences. In both circumstances, positive pore water pressures are generated at the depth of the potential slip surface, resulting in a reduction in the effective stress and consequently of the soil shear strength. This generally occurs in slopes consisting of layered soils, such as for instance a thin soil layer with a high permeability overlaying a much less permeable material or a fractured rock mass resting on an impervious bedrock [8–10]. Due to the high permeability of the upper layer, the slope response to rainfall is very rapid. Consequently, a single rain event may be sufficient to trigger a failure process.

Several empirical relationships have been proposed in the literature to relate rainfall intensity and duration to landslide occurrence [11–16]. Generally, these relationships are based on empirical observations (often at the regional scale). Therefore, some specific factors that strongly influence the slope response to rainfall, such as the slope geometry,

soil properties, and pore water pressures existing in the slope before rain, are not directly accounted for in these relationships. To overcome this limitation, theoretical and experimental studies have been performed to develop methods capable of relating landslide triggering to the hydro-mechanical properties of the soil and pore pressure regime of the slope [8,17–37]. Although numerical methods provide a comprehensive understanding of a failure process induced by the infiltration of rain into the slope, the availability of an effective and simple-to-use methodology directly relating rainfall to landslide occurrence would undoubtedly be a useful tool for a preliminary assessment of the slope stability conditions due to rainfall events. Moreover, using complex and computationally expensive methods (such as the numerical ones) cannot be completely justified when all required model parameters are not available.

In the present study, a method of practical interest was developed to predict the occurrence of very shallow landslides (generally, 1–2 m thick) due to rain infiltration that generates positive pore water pressures within the slope. A relationship is also provided to establish when this condition occurs and hence when the proposed method can be employed. Specifically, this method uses a closed-form solution to evaluate the change in pore water pressure caused by rain infiltration and the simple scheme of infinite slope to calculate the critical value of the pore water pressure that determines the incipient failure condition of the slope. In this way, a threshold curve is derived to readily predict landslide triggering due to expected rainfall scenarios. Only a few parameters are required as input data, which can be easily obtained from conventional geotechnical tests. As an example, the method is used to analyze a well-documented case study published in the literature.

2. Proposed Method

The model presented in this section is based on the following simplified assumptions: perfect synchronism between rainfall and groundwater-level fluctuations, the porosity and saturation degree of the portion of the soil above the groundwater level are constant, and the slope can be schematized using the simple scheme of infinite slope characterized by the presence of a thin soil layer resting on a less permeable material (Figure 1). This slope makes an angle α with the horizontal plane and eventually accommodates groundwater within it. In this latter case, the slope is subjected to seepage parallel to the ground surface.

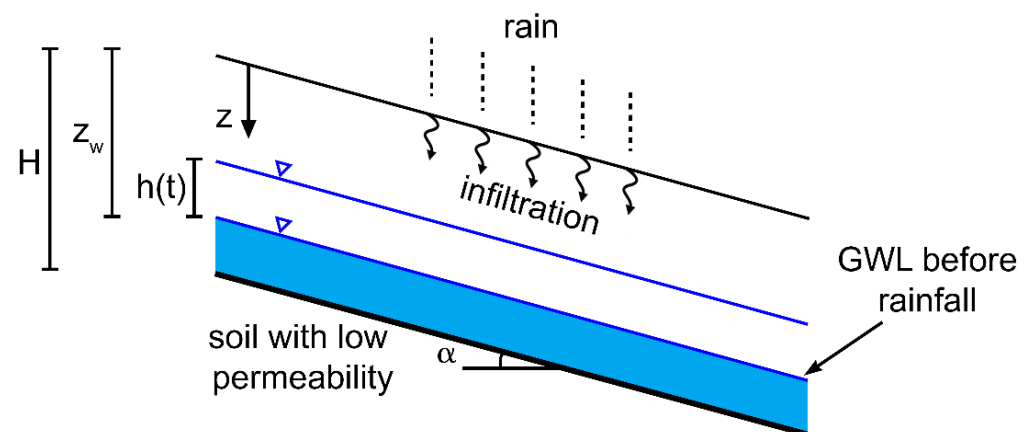


Figure 1. Scheme of infinite slope consisting of a cover layer on a less permeable soil, with $h(t)$ indicating the change in the groundwater level (GWL) due to rain infiltration.

In Figure 1, z is the depth, H is the thickness of the upper soil layer, z_w is the depth of the initial groundwater level, and $h(t)$ is the change in the groundwater level due to rain infiltration. All these quantities are measured in the vertical direction. Generally, a potential slip surface develops at the base of the upper soil layer ($z = H$), but this is not a restriction for the proposed method.

The condition for the use of this method can be analytically expressed by the following inequality (see Appendix A):

$$\cos^2 \alpha (\tan \alpha - \tan \phi') - \frac{c'}{\gamma z} < 0 \quad (1)$$

in which γ is the soil unit weight, and c' and ϕ' are the effective cohesion and the angle of shearing resistance of the soil, respectively. This inequality derives from the expression of the safety factor for an infinite slope when the effect of the initial pore water pressures is ignored and the slope is stable. Equation 1 implies that a landslide can be triggered only if positive pore water pressures are generated at the potential failure surface due to the formation of a water table or a rise in the existing groundwater level within the slope. In contrast, if the inequality in Equation (1) is not fulfilled, the slope is unstable when the pore water pressure at the potential failure surface is ignored. This means that the stability of the slope is ensured by the presence of an initial negative pore pressure (suction) that may become nil due to rain infiltration. In this case, the present method is unsuitable and a different approach should be used [38]. For cohesionless soils, Equation (1) reduces to

$$\tan \phi' > \tan \alpha \quad (2)$$

Referring to a given period of rainfall with a constant intensity R and duration d , the infiltration rate, I , is evaluated in the present study as follows:

$$I = R \text{ if } R < p \quad (3a)$$

$$I = p \text{ if } R \geq p \quad (3b)$$

where p is the potential infiltration rate, i.e., the maximum volume of water (per unit area) that can infiltrate into the slope in a unit of time. Generally, a determination of p is very complicated because it is affected by many factors that are difficult to be accounted for in the analysis, such as evapotranspiration, antecedent rainfall, vegetation, superficial cracks, and preferential drainage pathways [39,40]. For practical purposes, it is convenient to consider an operative value of p that should be evaluated on the basis of the results of field infiltration tests, taking into account the rainfall direction in relation to the slope inclination. In the absence of these data and especially when wet conditions occur, the following approximate equation may be used under the assumption that the rainfall is in the vertical direction [26]:

$$p = k \cos \alpha \quad (4)$$

where k is the saturated hydraulic conductivity of the soil. This assumption should also result in the maximum water infiltration because k is the greatest hydraulic conductivity of the soil. As a result, the water volume (per unit area) that is stored in the soil at time t is given by the product of I by t . Under the assumption of perfect synchronism between the rainfall and the groundwater level change, $h(t)$ can be written as

$$h(t) = \frac{I t}{n (1 - S_r)} \quad (5)$$

where n and S_r are, respectively, the porosity and degree of saturation of the soil above the groundwater level. An evaluation of these parameters can be performed by measurements of dilatational and shear wave velocities (V_P and V_S) as proposed by [41,42]. In the present study, these soil parameters are assumed to be constant for simplicity, considering also that the present method only concerns shallow landslides with a small thickness. Equation (5) is valid when $S_r < 1$, i.e., rain cannot infiltrate through the ground surface when the soil is completely saturated ($S_r = 1$) and, consequently, $h(t) = 0$ is imposed. After the rainfall event end (i.e., for $t > d$), the groundwater level decreases due to seepage occurring in the

saturated portion of the slope. The associated change in the water level may be calculated as follows [29]:

$$h(t) = h_{\max} e^{-k_T \sin \alpha \cos \alpha (t-d)} \tag{6}$$

where k_T is a model parameter that should be calibrated on the basis of rain recordings and groundwater level measurements. Montrasio and Valentino [18] derived a similar equation and suggested assuming a value of k_T that is slightly greater than k . As an example, function $h(t)$ is plotted in Figure 2 for different values of k_T . As can be seen, the maximum increase in the water level, h_{\max} , does not depend on k_T . Specifically, h_{\max} occurs at the end of the rainfall event (Figure 2) and can be hence calculated imposing that $t = d$ in Equation (5), with h_{\max} not exceeding z_w (Figure 1). Finally, the maximum value of the change in the pore water pressure is

$$u_{\max} = \gamma_w h_{\max} \cos^2 \alpha = \gamma_w \frac{I d}{n (1 - S_r)} \cos^2 \alpha \tag{7}$$

where γ_w is the unit weight of water.

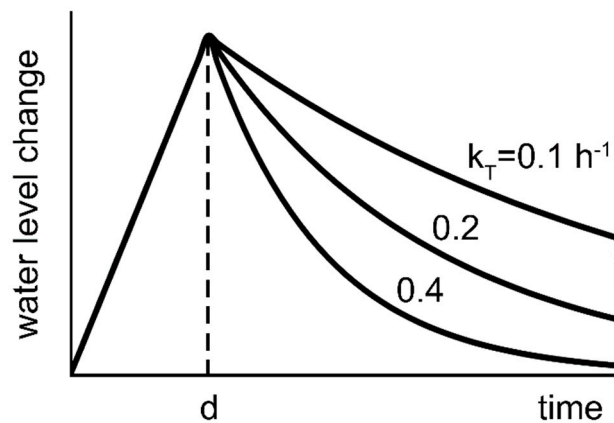


Figure 2. Example of the calculated change in the groundwater level due to rain infiltration.

A slope failure occurs when u_{\max} equals or exceeds a critical threshold, u_c , at a given depth. This latter value can be derived by equaling the safety factor of the slope, SF , (calculated at the same depth) to unity, i.e.,

$$SF = \frac{c' + (\gamma z \cos^2 \alpha - u_{w0} - u_c) \tan \phi'}{\gamma z \sin \alpha \cos \alpha} = 1 \tag{8}$$

where u_{w0} is the pore water pressure existing at the considered depth before rainfall commences, which hence accounts for the effect of the antecedent precipitations on the slope stability. In unsaturated soils, u_{w0} takes a negative value (suction) that can be measured by installing tensiometers in the slope. In these circumstances, landslide triggering is caused by the formation of a water table that generates positive pore water pressures within the slope. In contrast, if the potential slip surface is initially submerged in water (Figure 1), u_{w0} is positive and can be evaluated using the equation:

$$u_{w0} = \gamma_w (z - z_w) \cos^2 \alpha \tag{9}$$

In this latter case, failure may be triggered by an increase in the pore water pressure due to a rise in the groundwater level. Solving Equation (8), the expression of u_c is obtained as follows:

$$u_c = \frac{1}{\tan \phi'} [c' - u_{w0} \tan \phi' + \gamma z \cos \alpha (\cos \alpha \tan \phi' - \sin \alpha)] \tag{10}$$

Finally, the following relationship is derived from Equation (7), in which it is imposed that $u_{\max} = u_c$:

$$d_{\text{crit}} = \frac{n (1 - S_r) u_c}{\gamma_w \cos^2 \alpha} I^{-1} \tag{11}$$

where d_{crit} defines the duration of an infiltration process with intensity I , which is capable of triggering a slope failure at the depth considered. This critical duration also coincides with the time when the slope failure occurs. Equation (11) describes a hyperbola relating d_{crit} to I , with this latter provided by Equations (3a) and (3b). Consequently, d_{crit} reduces with increasing I . This implies that a rainfall event with a short duration may trigger a landslide if it is characterized by a high infiltration rate. In contrast, a rainfall event characterized by a low infiltration rate may trigger a landslide if it is sufficiently prolonged with time. In addition, considering that the infiltration rate is limited from above by p , a lower bound of the rainfall duration, d_{min} , can be calculated by imposing $I = p$ in Equation (11), i.e.,

$$d_{\text{min}} = \frac{n (1 - S_r) u_c}{\gamma_w \cos^2 \alpha} p^{-1} \tag{12}$$

An evaluation of d_{min} is very useful from a practical viewpoint, because no landslide is triggered at the considered depth for rain duration less than d_{min} .

By plotting Equation (11) for different values of I (with $0 < I \leq p$), a critical curve can be obtained. An example of this curve is shown in Figure 3. It defines the precipitations potentially capable of triggering a shallow landslide at an established depth where the initial pore water pressure is known.

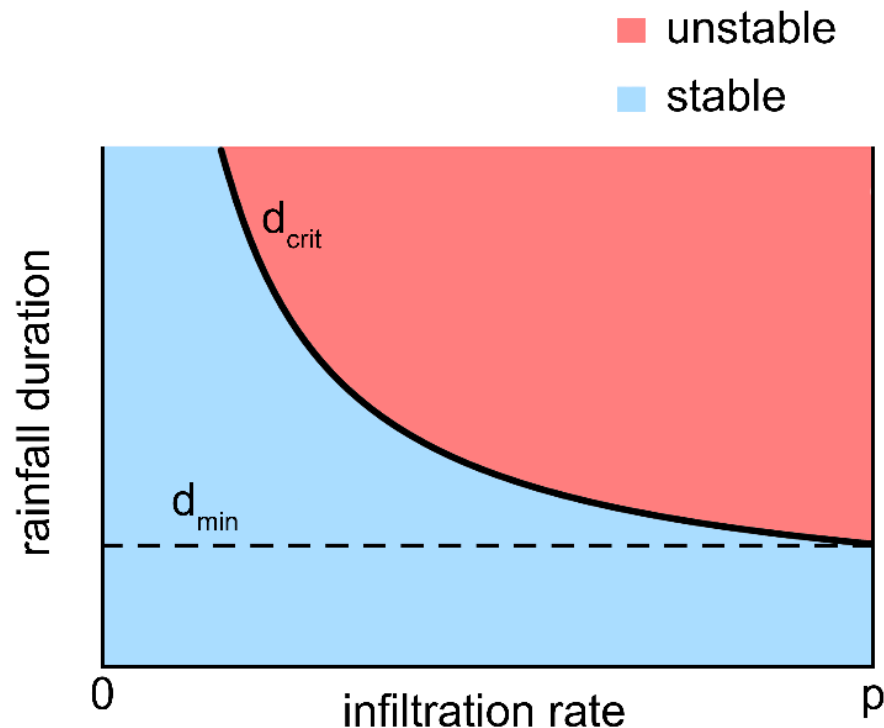


Figure 3. Example of a critical curve defining the precipitations capable of triggering a shallow landslide at a given depth.

Specifically, if the point representative of an expected rainfall event (with infiltration rate I and duration d) falls into the region above the critical area (highlighted in red in Figure 3), a landslide is triggered (at $t = d_{\text{crit}}$) due to the formation of a water table or an increase in the pre-existing groundwater level. Otherwise, the slope is stable.

3. Application of the Method to a Case Study

As an example, the proposed method is used in this section to analyze a rainfall-induced shallow landslide that affected a slope located in the area of Oltrepò Pavese (Northern Italy). This landslide was documented by Bordoni et al. [43,44] and Montrasio et al. [45]. The slope consisted of a cover soil of clayey–sandy silt with a thickness of about 1.40 m resting on bedrock (Figure 4).

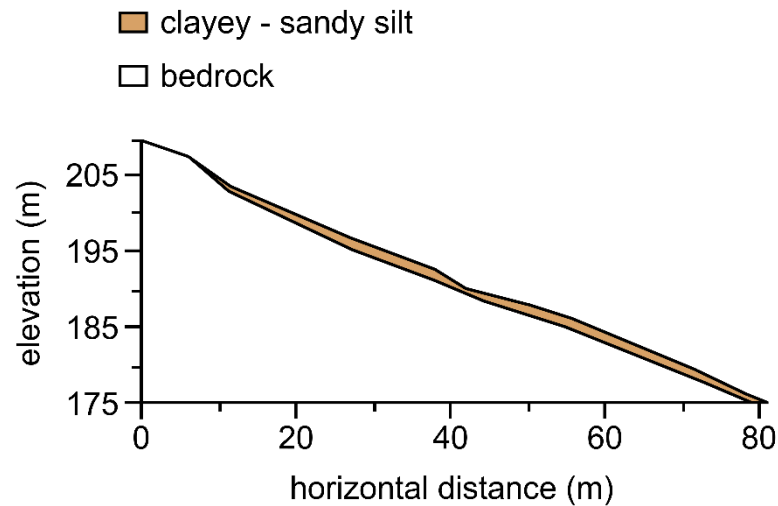


Figure 4. Geological model of the slope considered in the analysis (adapted from [44]).

Several tensiometers and TDR sensors were installed at different depths within the slope [43–45]. A rain gauge station was also installed. Long-term measurements of pore water pressure, water content, and rainfall depth are available. According to the available monitoring data, during the wet periods a water table usually forms in the lower portion of the cover soil (Figure 5) where the permeability is reduced due to the high content of carbonates [44].

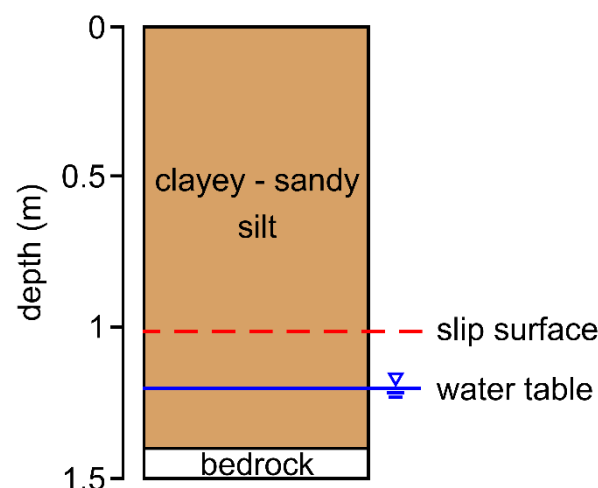


Figure 5. Soil profile of the considered site, indicating the location of the observed water table and that of the slip surface (adapted from [44]).

The slope can be schematized as an infinite slope with $\alpha = 30^\circ$, made up of a clayey–sandy silt. Triaxial tests performed on undisturbed samples provided $\phi' = 33^\circ$ with no effective cohesion. However, values of $c' = 29$ kPa and $\phi' = 26^\circ$ were found in the lower portion of the cover soil, at a depth of about 1.2 m from the ground surface. This high value of c' ensures that the slope is stable at this depth, even when a water table forms in the cover

layer. Other available soil parameters are $k = 1.5 \cdot 10^{-6}$ m/s, $\gamma = 16.8$ kN/m³, $n = 0.47$, and $S_r = 0.7$ [43–45]. Since no infiltration test was carried out, the potential infiltration rate was approximately evaluated using Equation (4), resulting in $p = 4.68$ mm/h. Rainfall recordings from June 2012 to November 2014 are plotted in Figure 6.

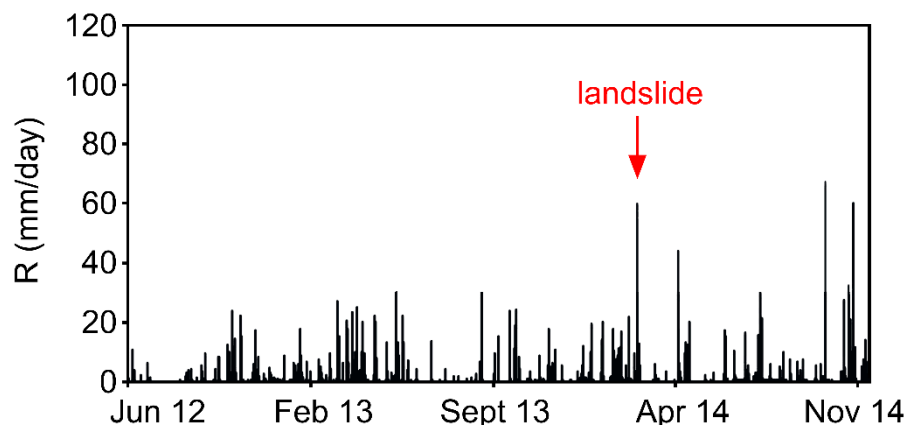


Figure 6. Daily rainfall recorded from June 2012 to November 2014 at the considered site (modified from [45]).

During this observation period, a shallow landslide was triggered at the beginning of March 2014 (Figure 6) with a slip surface located at a depth of 1 m from the ground surface (Figure 5). Considering that the soil is cohesionless at this depth and $\phi' > \alpha$ (Equation (2)), the landslide would have been triggered by an increase in the water table located at a depth of about 1.2 m (Figure 5). Five rainfall events, denoted E1, E2, E3, E4, and E5, are considered as indicated in Table 1, because all data required by the proposed method are available only for these events [43–45]. The date, intensity, and duration of each event are summarized in Table 1 along with the measured values of u_{wo} [44].

Table 1. Date, rainfall intensity, duration, and initial pore pressure for the rain events considered in the present study (data drawn from [43]).

Event	Date	R (mm/h)	d (h)	u_{wo} (kPa)
E1	24–25 March 2013	1.24	24	−0.65
E2	30 March 2013	1.90	13	−0.50
E3	20–22 April 2013	0.90	54	−1.60
E4	18–20 January 2014	0.80	44	−1.20
E5	28 February–2 March 2014	1.60	43	−0.70

Considering that the values of u_{wo} are negative, the slip surface developed in a portion of the slope that was initially unsaturated. Since the intensity R of each rain event is less than the potential infiltration rate p , rain completely infiltrated into the slope according to Equations (3a)–(3b). Table 2 presents the values of u_c and d_{min} calculated using Equations (10) and (12), respectively.

Table 2. Calculated values of u_c and d_{min} for each rain event considered.

Event	u_c (kPa)	d_{min} (h)
E1	2.05	8.2
E2	1.90	7.6
E3	3.00	12.1
E4	2.60	10.4
E5	2.10	8.4

From these results, it can be inferred that no landslide was triggered by a rainfall event with a duration of less than 7 h, and a small change in the pore water pressure (2–3 kPa) is sufficient to cause a slope failure at the depth of the observed slip surface ($z = 1$ m). Figures 7 and 8 show the critical curves calculated using Equation (11) along with the measured values of u_{wo} presented in Table 1.

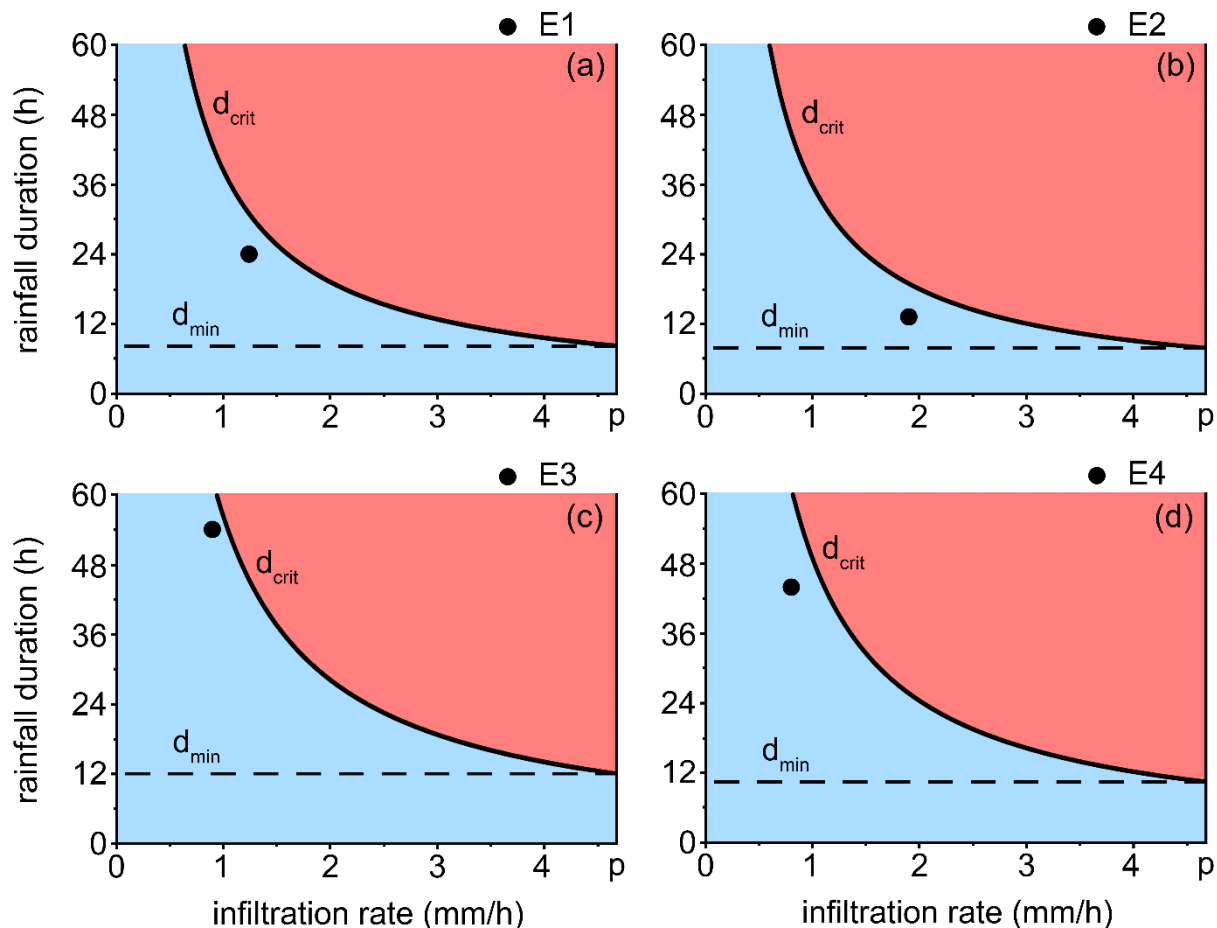


Figure 7. Critical curve calculated at the depth of the slip surface where (a) $u_{wo} = -0.65$ kPa; (b) $u_{wo} = -0.50$ kPa; (c) $u_{wo} = -1.60$ kPa; and (d) $u_{wo} = -1.20$ kPa. The black points represent the rain events E1, E2, E3 and E4.

The points representative of the considered rainfall events are also plotted in these figures. Although the duration of E1, E2, E3, and E4 is greater than d_{min} , the associated points are located below the respective critical curves (Figure 7). As a result, the slope remains stable after these rainfall events. By contrast, the point representing the fifth event (E5) is located above the critical curve and hence it falls into the region where the slope is not stable (Figure 8). These results are consistent with what was actually observed, i.e., a landslide was triggered by the last rainfall event, whereas no failure was observed after the other events considered. In addition, as predicted by Equation (5), the last event caused an increase in the groundwater level of about 50 cm, owing to which the level rose above the depth of the slip surface (Figure 5), producing a positive pore water pressure at this depth. Finally, Equation (11) allows us to assert that a failure occurred about 24 h after the beginning of E5 (i.e., on 1 March 2014). These results are in accord with what is documented in the studies by Bordoni et al. [43,44] and Montrasio et al. [45].

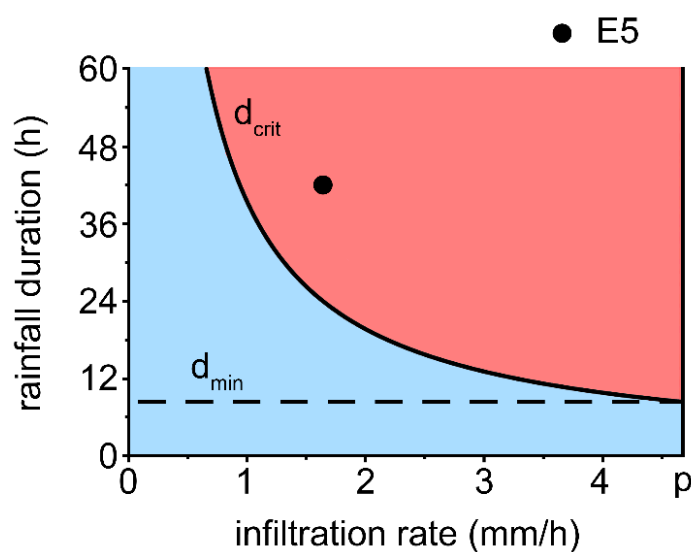


Figure 8. Critical curve calculated at the depth of the slip surface where $u_{w0} = -0.70$ kPa, with the point representing the rainfall event E5.

4. Conclusions

A method of practical interest is proposed in the present study for a preliminary prediction of the occurrence of shallow landslides (generally 1–2 m thick) triggered by the positive pore water pressures generated within the slope owing to rainfall. This occurs, for instance, when a water table forms or when the existing groundwater level rises within the slope. On the basis of the simple scheme of infinite slope and using some closed-form expressions, an analytical threshold curve was obtained for assessing whether an expected rainfall event with a given intensity and duration is capable of triggering a slope failure at the potential slip surface, where the existing (negative or positive) pore pressure is known. This threshold curve is formally similar to several empirical rainfall intensity–duration relationships available in the literature. However, unlike these relationships, the proposed solution explicitly depends on the slope geometry, pre-existing pore water pressure, and soil properties at the local scale. In addition, some useful parameters can also be estimated, such as the minimum rain duration capable of triggering a landslide or the time of failure. The proposed method is very simple to use and only requires a few soil parameters as input data, which can be obtained from conventional tests. Therefore, it appears to be very attractive from a practical viewpoint. Nevertheless, a more extensive validation will be required in the future.

Author Contributions: Conceptualization, A.T., L.P. and E.C.; Writing—original draft, A.T., L.P. and E.C.; Writing—review & editing, A.T., L.P. and E.C. All authors have read and agreed to the published version of the manuscript.

Funding: This research was funded by “Fondo Sociale Europeo REACT-EU Programma Operativo Nazionale (PON) Ricerca e Innovazione 2014–2020”.

Data Availability Statement: The data presented in this study are available on request from the corresponding author.

Conflicts of Interest: The authors declare no conflict of interest.

Appendix A

The mechanism of collapse considered in the present study (i.e., a shallow landslide triggered by the formation of a water table within the slope, with the consequent generation of positive pore water pressures) can occur only if the slope safety factor (evaluated neglecting any effect of the pore water pressure), SF_d , is greater than unity. Referring to

an infinite slope making an angle α with the horizontal direction, this condition can be expressed using the following equation:

$$SF_d = \frac{c' + \gamma z \cos^2 \alpha \tan \phi'}{\gamma z \sin \alpha \cos \alpha} > 1 \quad (\text{A1})$$

Equation (A1) can be manipulated as follows:

$$c' + \gamma z \cos^2 \alpha \tan \phi' > \gamma z \sin \alpha \cos \alpha \quad (\text{A2})$$

$$\sin \alpha \cos \alpha - \cos^2 \alpha \tan \phi' - \frac{c'}{\gamma z} < 0 \quad (\text{A3})$$

$$\cos^2 \alpha (\tan \alpha - \tan \phi') - \frac{c'}{\gamma z} < 0 \quad (\text{A4})$$

References

- Campbell, R.H. *Soil Slips, Debris Flows, and Rainstorms in the Santa Monica Mountains and Vicinity, Southern California*; Series number 851; Professional Paper; US Geological Survey: Alexandria, VA, USA, 1975.
- Eckersley, D. Instrumented laboratory flow slides. *Géotechnique* **1990**, *40*, 489–502. [[CrossRef](#)]
- Cruden, D.M.; Varnes, D.J. *Landslides—Investigation and Mitigation*; Special report No. 247, Transportation Research Board; National Academy Press: Washington, DC, USA, 1996.
- Hungr, O.; Evans, S.G.; Bovis, M.J.; Hutchinson, J.N. A review of the classification of landslides of the flow type. *Environ. Eng. Geosci.* **2001**, *7*, 221–238. [[CrossRef](#)]
- Olivares, L.; Picarelli, L. Shallow flowslides triggered by intense rainfalls on natural slopes covered by loose unsaturated pyroclastic soils. *Géotechnique* **2003**, *53*, 283–287. [[CrossRef](#)]
- Cascini, L.; Cuomo, S.; Sorbino, G. Flow-like mass movements in pyroclastic soils: Remarks on the modelling of triggering mechanisms. *Ital. Geotech. J.* **2005**, *39*, 11–31.
- Picarelli, L.; Olivares, L.; Comegna, L.; Damiano, E. Mechanical aspects of flow-like movements in granular and fine grained soils. *Rock Mech. Rock Eng.* **2008**, *41*, 179–197. [[CrossRef](#)]
- Godt, J.W.; Baum, R.L.; Savage, W.Z.; Salciarini, D.; Schulz, W.H.; Harp, E.L. Transient deterministic shallow landslide modeling: Requirements for susceptibility and hazard assessments in a GIS framework. *Eng. Geol.* **2008**, *102*, 214–226. [[CrossRef](#)]
- Kelln, C.J.; Barbour, S.L.; Qualizza, C. Fracture-dominated Subsurface Flow and Transport in a Sloping Reclamation Cover. *Vadose Zone J.* **2009**, *8*, 96–107. [[CrossRef](#)]
- Baum, R.L.; Godt, J.W.; Savage, W.Z. Estimating the timing and location of shallow rainfall-induced landslides using a model for transient, unsaturated infiltration. *J. Geophys. Res.* **2010**, *115*, F03013. [[CrossRef](#)]
- Caine, N. The rainfall intensity-duration control of shallow landslides and debris flows. *Geogr. Ann. A* **1980**, *62*, 23–27.
- Wieczorek, G.F.; Glade, T. Climatic factors influencing occurrence of debris flows. In *Debris-Flow Hazard and Related Phenomena*; Jakob, M., Hungr, O., Eds.; Springer: Berlin/Heidelberg, Germany, 2005; pp. 325–362.
- Guzzetti, F.; Peruccacci, S.; Rossi, M.; Stark, C.P. Rainfall thresholds for the initiation of landslides in central and southern Europe. *Meteorol. Atmos. Phys.* **2007**, *98*, 239–267. [[CrossRef](#)]
- Baum, R.L.; Godt, J.W. Early warning of rainfall-induced shallow landslides and debris flows in the USA. *Landslides* **2010**, *7*, 259–272. [[CrossRef](#)]
- Ponziani, F.; Pandolfo, C.; Stelluti, M.; Berni, N.; Brocca, L.; Moramarco, T. Assessment of rainfall thresholds and soil moisture modeling for operational hydrogeological risk prevention in the Umbria region (central Italy). *Landslides* **2012**, *9*, 229–237. [[CrossRef](#)]
- Peruccacci, S.; Brunetti, M.T.; Gariano, S.L.; Melillo, M.; Rossi, M.; Guzzetti, F. Rainfall thresholds for possible landslide occurrence in Italy. *Geomorphology* **2017**, *290*, 39–57. [[CrossRef](#)]
- Crosta, G.B. Regionalization of rainfall thresholds: An aid to landslide hazard evaluation. *Environ. Geol.* **1998**, *35*, 131–145. [[CrossRef](#)]
- Montrasio, L.; Valentino, R. Experimental analysis and modelling of shallow landslides. *Landslides* **2007**, *4*, 291–296. [[CrossRef](#)]
- Van Asch, T.W.J.; Van Beek, L.P.H.; Bogaard, T.A. Problems in predicting the mobility of slow-moving landslides. *Eng. Geol.* **2007**, *91*, 46–55. [[CrossRef](#)]
- Borja, R.I.; White, J.A. Continuum deformation and stability analyses of a steep hillside slope under rainfall infiltration. *Acta Geotech.* **2010**, *5*, 1–14. [[CrossRef](#)]
- Cascini, L.; Cuomo, S.; Pastor, M.; Sorbino, G. Modeling of Rainfall-Induced Shallow Landslides of the Flow Types. *J. Geotech. Geoenviron. Eng. ASCE* **2010**, *136*, 85–98. [[CrossRef](#)]
- Pagano, L.; Picarelli, L.; Rianna, G.; Urciuoli, G. A simple numerical procedure for timely prediction of precipitation-induced landslides in unsaturated pyroclastic soils. *Landslides* **2010**, *7*, 273–289. [[CrossRef](#)]

23. Conte, E.; Troncone, A. Analytical Method for Predicting the Mobility of Slow-Moving Landslides owing to Groundwater Fluctuations. *J. Geotech. Geoenviron. Eng. ASCE* **2011**, *137*, 777–784. [[CrossRef](#)]
24. Conte, E.; Troncone, A. Stability analysis of infinite clayey slopes subjected to pore pressure changes. *Géotechnique* **2012**, *62*, 87–91. [[CrossRef](#)]
25. Conte, E.; Troncone, A. A method for the analysis of soil slips triggered by rainfall. *Géotechnique* **2012**, *62*, 187–192. [[CrossRef](#)]
26. Conte, E.; Troncone, A. Simplified approach for the analysis of rainfall-induced shallow landslides. *J. Geotech. Geoenviron. Eng. ASCE* **2012**, *138*, 398–406. [[CrossRef](#)]
27. Damiano, E.; Olivares, L.; Picarelli, L. Steep-slope monitoring in unsaturated pyroclastic soils. *Eng. Geol.* **2012**, *137–138*, 1–12. [[CrossRef](#)]
28. Hungr, O.; Leroueil, S.; Picarelli, L. The Varnes classification of landslide types, an update. *Landslides* **2014**, *11*, 167–194. [[CrossRef](#)]
29. Conte, E.; Donato, A.; Troncone, A. A simplified method for predicting rainfall-induced mobility of active landslides. *Landslides* **2017**, *14*, 35–45. [[CrossRef](#)]
30. Lizárraga, J.J.; Frattini, P.; Crosta, G.B.; Buscarnera, G. Regional-scale modelling of shallow landslides with different initiation mechanisms: Sliding versus liquefaction. *Eng. Geol.* **2017**, *228*, 346–356. [[CrossRef](#)]
31. Salciarini, D.; Fanelli, G.; Tamagnini, C. A probabilistic model for rainfall-induced shallow landslide prediction at the regional scale. *Landslides* **2017**, *14*, 1731–1746. [[CrossRef](#)]
32. Askarnejad, A.; Akca, D.; Springman, S.M. Precursors of instability in a natural slope due to rainfall: A full-scale experiment. *Landslides* **2018**, *15*, 1745–1759. [[CrossRef](#)]
33. Sun, J.; Huang, Y. Modeling the Simultaneous Effects of Particle Size and Porosity in Simulating Geo-Materials. *Materials* **2022**, *15*, 1576. [[CrossRef](#)]
34. Herath, H.M.J.M.K.; Kodagoda Sudheera, S.I.; Dias, A.A.V. *Shallow Modes of Slope Failure in Road Earth Cuttings in Sri Lanka*; Springer International Publishing: Berlin/Heidelberg, Germany, 2014. Available online: https://link.springer.com/chapter/10.1007/978-3-319-05050-8_9#copyright-information (accessed on 29 August 2022).
35. Troncone, A.; Conte, E.; Pugliese, L. Analysis of the Slope Response to an Increase in Pore Water Pressure Using the Material Point Method. *Water* **2019**, *11*, 1446. [[CrossRef](#)]
36. Troncone, A.; Pugliese, L.; Lamanna, G.; Conte, E. Prediction of rainfall-induced landslide movements in the presence of stabilizing piles. *Eng. Geol.* **2021**, *288*, 106143. [[CrossRef](#)]
37. Troncone, A.; Pugliese, L.; Parise, A.; Conte, E. Prediction of Slow-Moving Landslide Mobility Due to Rainfall Using a Two-Wedges Model. *Water* **2021**, *13*, 2030. [[CrossRef](#)]
38. Conte, E.; Pugliese, L.; Troncone, A. A Simple Method for Predicting Rainfall-Induced Shallow Landslides. *J. Geotech. Geoenviron. Eng. ASCE* **2022**, *148*, 04022079. [[CrossRef](#)]
39. Wilson, G.W.; Fredlund, D.G.; Barbour, S.L. Coupled soil-atmosphere modeling for soil evaporation. *Can. Geotech. J.* **1994**, *31*, 151–161. [[CrossRef](#)]
40. Blight, G.E. 37th Rankine Lecture: Interaction between the atmosphere and the Earth. *Géotechnique* **1997**, *47*, 713–767. [[CrossRef](#)]
41. Conte, E.; Cosentini, R.M.; Troncone, A. Shear and dilatational wave velocities for unsaturated soils. *Soil Dyn. Earthq. Eng.* **2009**, *29*, 946–952. [[CrossRef](#)]
42. Conte, E.; Cosentini, R.M.; Troncone, A. Geotechnical parameters from V_p and V_s measurements in unsaturated soils. *Soils Found.* **2009**, *49*, 689–698. [[CrossRef](#)]
43. Bordoni, M.; Meisina, C.; Valentino, R.; Bittelli, M.; Chersich, S. Site-specific to local-scale shallow landslides triggering zones assessment using TRIGRS. *Nat. Hazards Earth Syst. Sci.* **2015**, *15*, 1025–1050. [[CrossRef](#)]
44. Bordoni, M.; Meisina, C.; Valentino, R.; Lu, N.; Bittelli, M.; Chersich, S. Hydrological factors affecting rainfall-induced shallow landslides: From the field monitoring to a simplified slope stability analysis. *Eng. Geol.* **2015**, *193*, 19–37. [[CrossRef](#)]
45. Montrasio, L.; Valentino, R.; Meisina, C. Soil Saturation and Stability Analysis of a Test Site Slope Using the Shallow Landslide Instability Prediction (SLIP) Model. *Geotech. Geol. Eng.* **2018**, *36*, 2331–2342. [[CrossRef](#)]